The Ratio of the Direct Photon Production Cross Section at 630 GeV and at 1800 GeV

Michael Strauss
University of Oklahoma, Norman, OK

DØ NOTE # $XXXX$
Preliminary Version 0.1
December 13, 2000

Abstract

We measure the ratio of the isolated direct photon prodution cross section at $\sqrt{s}$ = 630 GeV/c^2 to that at $\sqrt{s}$ = 1800 GeV/c^2 for the central ($|\eta| < 0.9$) and forward ($1.6 < |\eta| < 2.5$) rapidity regions. We compare the result with next to leading order QCD predictions using CTEQ parton distribution functions.

1 Introduction

The results from the published Run 1A/1B direct photon cross section [2, 1] and the direct photon cross section at 630 GeV/c^2 [3] are combined in this note to give the ratio of the cross sections. The measurement of the ratio is less sensitive to common systematic uncertainties and gives an important comparison between data and theoretical predictions.

2 Analysis Additions

2.1 1800 GeV Results

The luminosity for the published Run 1A/1B cross sections is adjusted upward by 3.4% due to the E811 results.

2.2 High E_T Bins

In order to facilitate the measurement ratio in bins of $x_T = 2E_T/\sqrt{2}$, the highest E_T bins in the 630 GeV data were changed to exactly match those of the 1800 GeV data. The previous 630 GeV results had a single bin starting at $x_T = .0833$ and extending to an x_T value higher than the maximum 1800 GeV measurement. The new binning has two x_T bins with $.0833 < x_T < .0944$ and $.0944 < x_T < .1556$. For the 630 GeV data, we set the maximum E_T to be 49 GeV, or $x_T = 0.1556$, which corresponds with them maximum E_T of 140 GeV for the 1800 GeV data.

2.3 Tracking Efficiency

The method to determine the tracking efficiency for the 630 GeV analysis in DØ Note #3699 is different than that in the published 1800 GeV analysis. In addition, the uncertainty in the tracking efficiency is the largest systematic uncertainty in the EC region ($1.6 < |\eta| < 2.5$) in the 630 analysis. Therefore, we have redone the tracking efficiency using the same method as that used in the 1800 GeV analysis.

In the original 630 GeV analysis the charged track efficiency, (ϵ_d), was determined from the data using Z^0 decays. This efficiency was then used in the Monte Carlo allowing events with charged tracks to pass the "no track" cut. However, because certain events with charged tracks were rejected in the Monte Carlo during generation, it was expected that the number of events with charged tracks in the data may be higher than that determined from tracking efficiency alone. Consequently, the purity fit allowed for an additional contribution from events with charged tracks. This method would work extremely well if the actual background from events with charged tracks was *greater than or equal to* that determined from the Z^0 decays. However, if the actual background from events with charged tracks is *lower* than that estimated from Z^0 decays, a large systematic error may be introduced. Therefore, we have changed the method for determing the background from charged tracks to that used in the published 1A/1B result. The amount of background consisting of events with charged tracks which are not reconstructed, is completely determined by the fit to the purity distribution.

The purity with the new E_T bins described above, combined with fitting for the entire background from charged tracks is shown in Figs. 1 and 2 using the variable $\log(1+\log(1+E_1))$ as the discriminant in the CC and EC, respectively.

Applying the Run 1A/1B method to determine the charged track back-

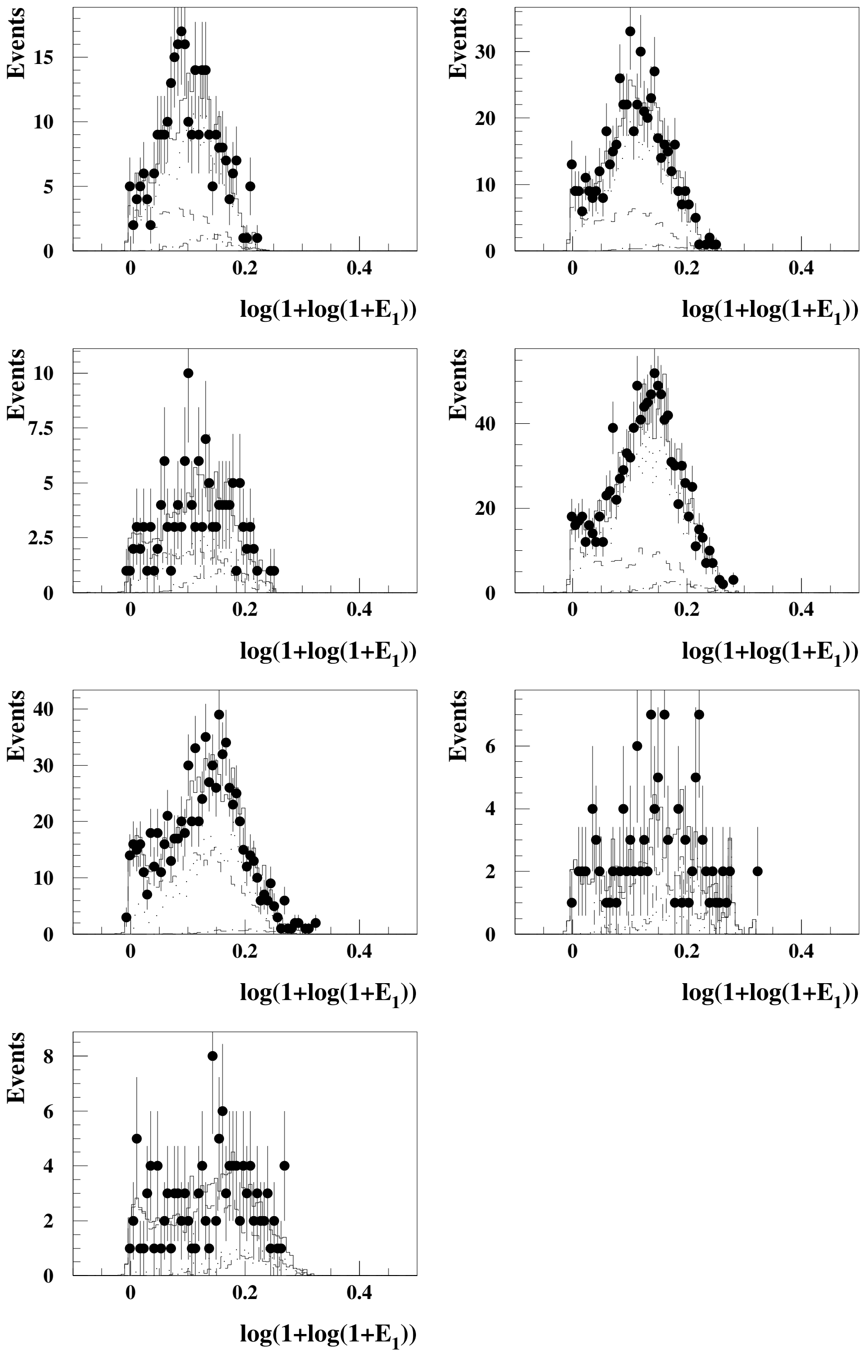

Figure 1: Distributions of $\log(1 + \log(1 + E_1))$ for the central η region in E_T bins of 7.35–9.10, 9.10–12.6, 12.6–14.7, 14.7–18.9, 18.9–26.25, 26.25–29.75, and >29.75 GeV. The solid line is total MC fit to the data. The dashed line is the photon contribution, the dotted line is the neutral jet background contribution, and the dash-dot line is the contribution from jets containing charged tracks.

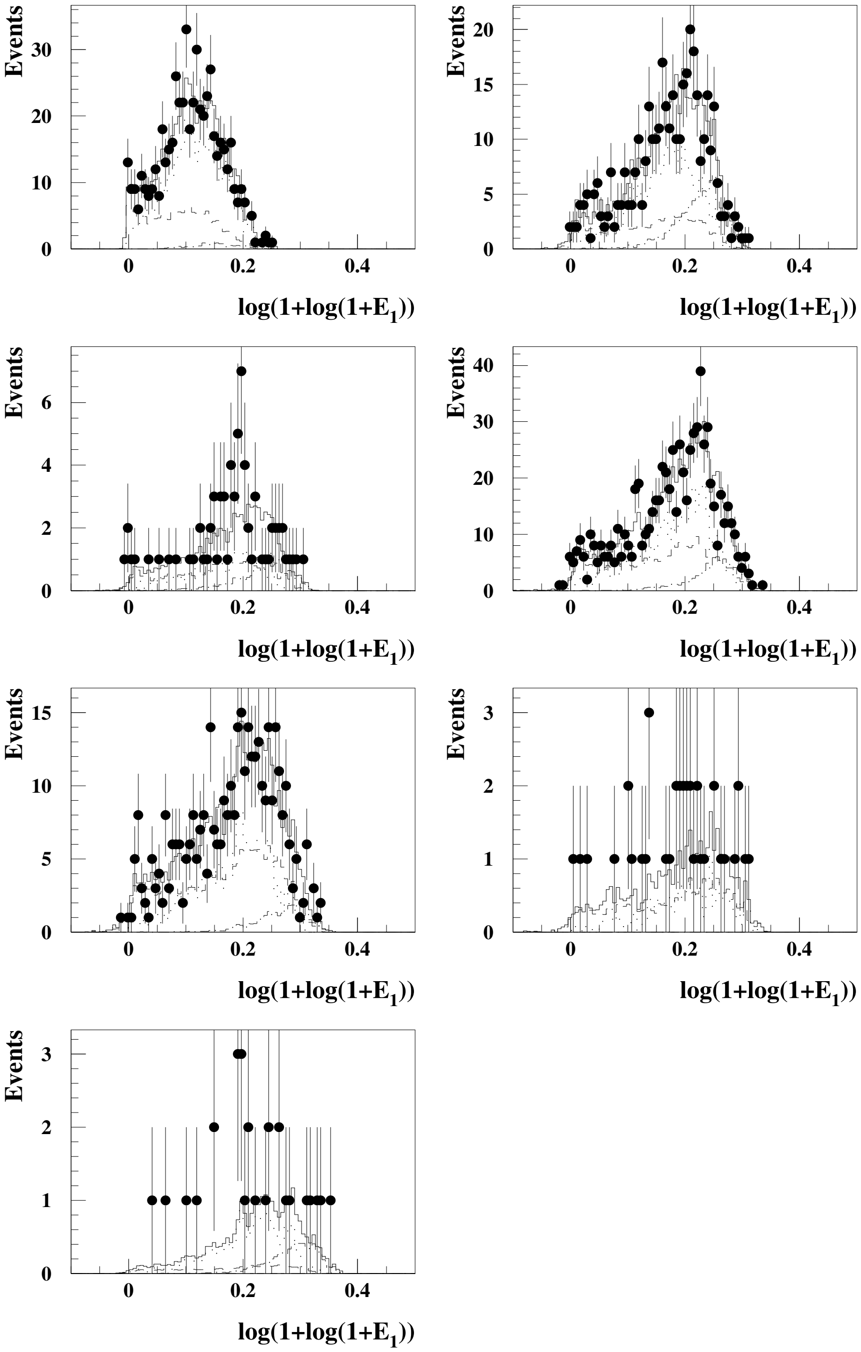

Figure 2: Distributions of $\log(1+\log(1+E_1))$ for the forward η region in E_T bins of 7.35–9.10, 9.10–12.6, 12.6–14.7, 14.7–18.9, 18.9–26.2, 26.25–29.75, and >29.75 GeV. The solid line is total MC fit to the data. The dashed line is the photon contribution, the dotted line is the neutral background contribution, and the dash-dot line is the contribution from jets containing charged tracks.

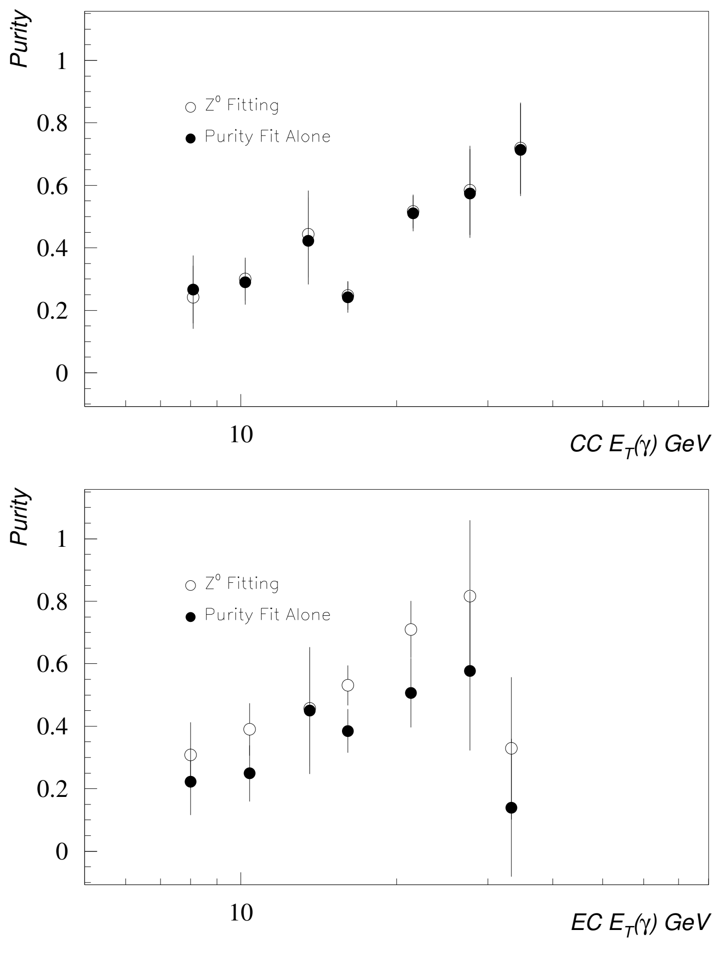

Figure 3: Photon purity using the tracking efficiency determined from Z^0 decays with extra track contributions compared to the purity with the track contribution determined entirely from the fit. The latter method is used in the Run 1A/1B analysis, and in the revised 630 analysis in this note.

ground has little effect on the final results for the CC ($|\eta| < 0.9$), but changes the results for the EC significantly as shown in Fig. 3. Each fitted purity bin in the EC has shifted to a lower value. It can be seen in Fig. 2 that signal events dominate the region at low $\log(1 + \log(1 + E_1))$, background events with charged tracks dominate the region at high $\log(1+\log(1+E_1))$, and neutral background events dominate the central region. When the charged and neutral backgrounds are fitted separately in the EC, the fraction of charged background events in the final sample is actually less than when that fraction is determined from Z^0 data. Because the fraction of neutral background is not constrained by the high tail (as it is whem the charged and neutral background are combined into one distribution), the fit prefers a much larger fraction of neutral background, thus decreasing the fraction of signal events.

The difference between the results of these two methods is completely compatible with a systematic error in the determination of the tracking efficiency from the Z^0 data. The uncertainty determined for the tracking efficency from the Z^0 data (σ_d) was the largest systematic uncertainty in DØ Note #3699, with a fractional uncertainty of 13%. We can compare the EC tracking efficiency of 0.593 ± 0.079 used in the previous note with the effective tracking efficiency calculated from the final fraction of charged tracks in the purity fit, (ϵ_f). The effective tracking efficiency is based on the ratio of the fraction of background events with charged tracks after the purity fit to the fraction of background events with charged tracks before the purity fit. This calculated tracking efficiency is consistently smaller than that determined from the Z^0 data. In Fig. 4, we plot the difference between the two methods for determing the tracking efficiency normalized by the error on the tracking efficiency, $(\epsilon_d - \epsilon_f)/\sigma_d$, which gives the number of standard deviations by which the two methods differ. The weighted average of the seven points is 3.6 ± 0.3 standard deviations.

We are not sure of the reason for this 3.6σ difference, but we can speculate as to a possible cause. The tracking efficiency determined from the Z^0 decays was parameterized as $\epsilon_d = (1 - pt)(1 - \psi)$ where p is the probability that a photon will convert before the tracking chambers, t is the probability that a track in the detector will be reconstructed, and ψ is the probability that a reconstructed track from the underlying event will be found in the tracking road of a good photon. The term ψ, which was found to be $.195 \pm .033 \pm .44$ in the EC for the Z^0 data at 1800 GeV may not be accurate for the data taken at 630 GeV. In particular, the luminosity was much lower in the 630 GeV data, which may give far fewer tracks from minimum bias events in the forward direction. The value of 19% corresponds somewhat with the difference in tracking efficiency determined from the Z^0 decays at 1800 GeV

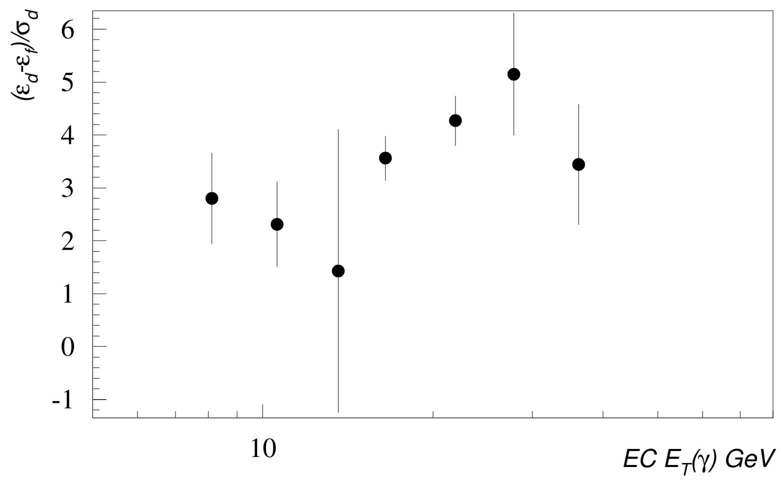

Figure 4: Number of standard deviations difference in the tracking efficiency determined from the purity fit and from Z^0 decays. The data is consistent with the tracking efficiency determined from z^0 decays being low by 3.6 standard deviations.

and from the purity fit at 630 GeV, which is about 20% at lower E_T and about 30% at higher E_T.

The purity with the fraction of charged track background determined from the purity fit and all other aspects of the analysis identical to that described in DØ Note #3699 is shown in Table 1 and Fig. 3. The purity divided by the efficiency is shown in Fig. 5.

E_TRange (GeV)	CC Fit	EC Fit
7.35-9.10	26.7 ± 10.9	22.2 ± 10.6
9.10-12.6	29.0 ± 7.2	24.9 ± 9.0
12.6-14.7	42.2 ± 13.9	45.0 ± 20.3
14.7-18.9	24.2 ± 4.9	38.5 ± 7.0
18.9-26.25	51.0 ± 5.7	50.7 ± 11.1
26.25-29.75	57.4 ± 14.2	57.7 ± 25.5
29.75-49.0	71.4 ± 14.8	13.9 ± 22.1

Table 1: Photon purity. In DØ Note #3699 the maximum E_T was not 49 GeV/c^2 and the highest two bins in this table were a single bin.

E_T Range (GeV)	E_T	$\frac{d\sigma}{dE_T}(\frac{\text{pb}}{\text{GeV}})$	$\delta\sigma_{\text{uncor}}(\%)$	$\delta\sigma_{\text{cor}}(\%)$
7.35- 9.1	8.2	47000	43	52
9.1-12.6	10.5	7160	26	36
12.6-14.7	13.6	2040	33	25
14.7-18.9	16.5	351	22	19
18.9-26.25	22.1	131	11	13
26.25-29.75	27.9	42.6	25	10
29.25-49.0	36.9	10.5	21	7

Table 2: Differential cross section in the CC with uncorrelated and correlated errors.

The measured cross section is shown in Fig. 6 along with a theoretical prediction using CTEQ4M as implemented by Owens *et. al.* [4]. Fig. 7 shows the difference between the experimental and theoretical differential cross sections. The correlated uncertainty includes contributions from the uncertainty on the geometric acceptance, the luminosity, the energy scale, and the fragmentation model. The uncorrelated uncertainty includes the uncertainties

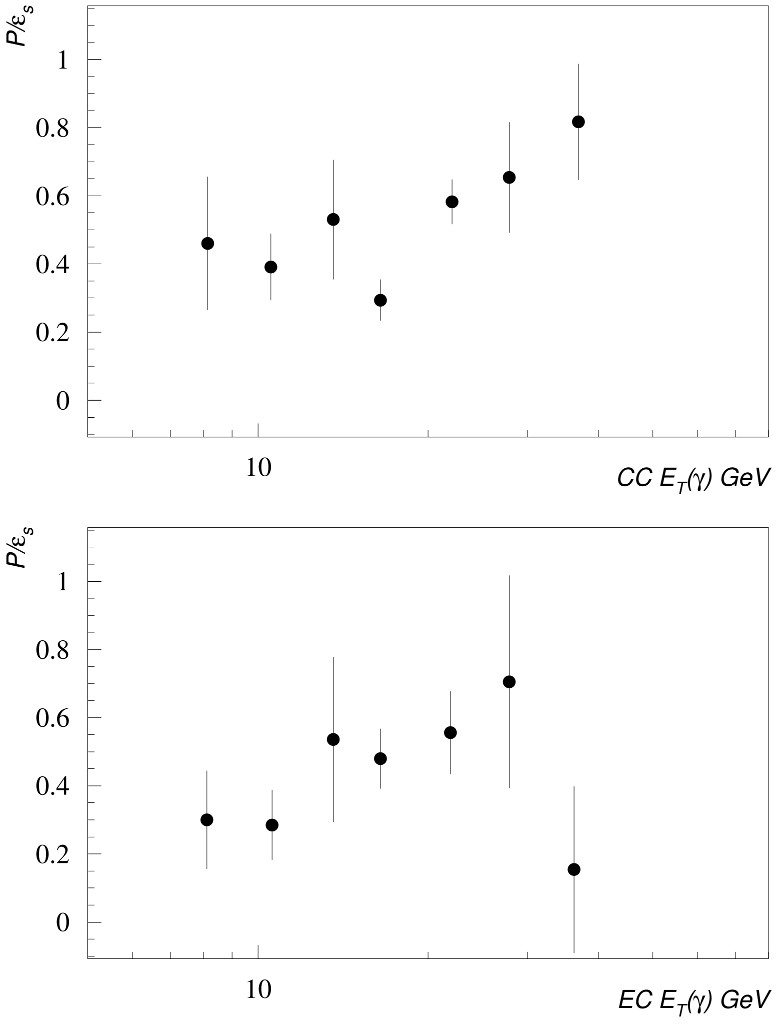

Figure 5: Photon purity divided by efficiency for the central and forward regions.

E_T **Range**	*Uncorrelated*			*Correlated*			
	$\mathcal{P}$	ϵ_s	**Trg**	**Frg**	**Esc**	**Act**	**Lum**
7.35- 9.1	41	12	6	51	6	1	4
9.1-12.6	25	2	6	36	5	1	4
12.6-14.7	33	2	1	24	3	1	4
14.7-18.9	20	2	8	18	3	1	4
18.9-26.25	11	1	1	12	2	1	4
26.25-29.75	25	2	0	9	2	1	4
29.75-49.0	21	1	0	6	2	1	4

Table 3: Sources of uncertainty in the CC (in percent).

E_T **Range (GeV)**	E_T	$\frac{d\sigma}{dE_T}(\frac{\text{pb}}{\text{GeV}})$	$\delta\sigma_{\text{uncor}}(\%)$	$\delta\sigma_{\text{cor}}(\%)$
7.35- 9.1	8.1	21800	48	30
9.1-12.6	10.6	3600	36	25
12.6-14.7	13.6	1290	45	21
14.7-18.9	16.5	420	19	18
18.9-26.3	21.9	66.4	22	15
26.25-29.75	27.8	17.5	44	13
29.75-49.0	36.2	0.512	160	11

Table 4: Differential cross section in the EC with uncorrelated and correlated errors.

E_T **Range**	*Uncorrelated*			*Correlated*			
	$\mathcal{P}$	ϵ_s	**Trg**	**Frg**	**Esc**	**Act**	**Lum**
7.35- 9.1	48	6	6	29	4	1	4
9.1-12.6	36	1	1	24	3	1	4
12.6-14.7	45	2	0	20	3	1	4
14.7-18.9	18	2	7	17	3	1	4
18.9-26.3	22	1	1	14	2	1	4
26.25-29.75	44	2	0	12	2	1	4
29.75-49.0	160	1	0	10	2	1	4

Table 5: Sources of uncertainty in the EC (in percent).

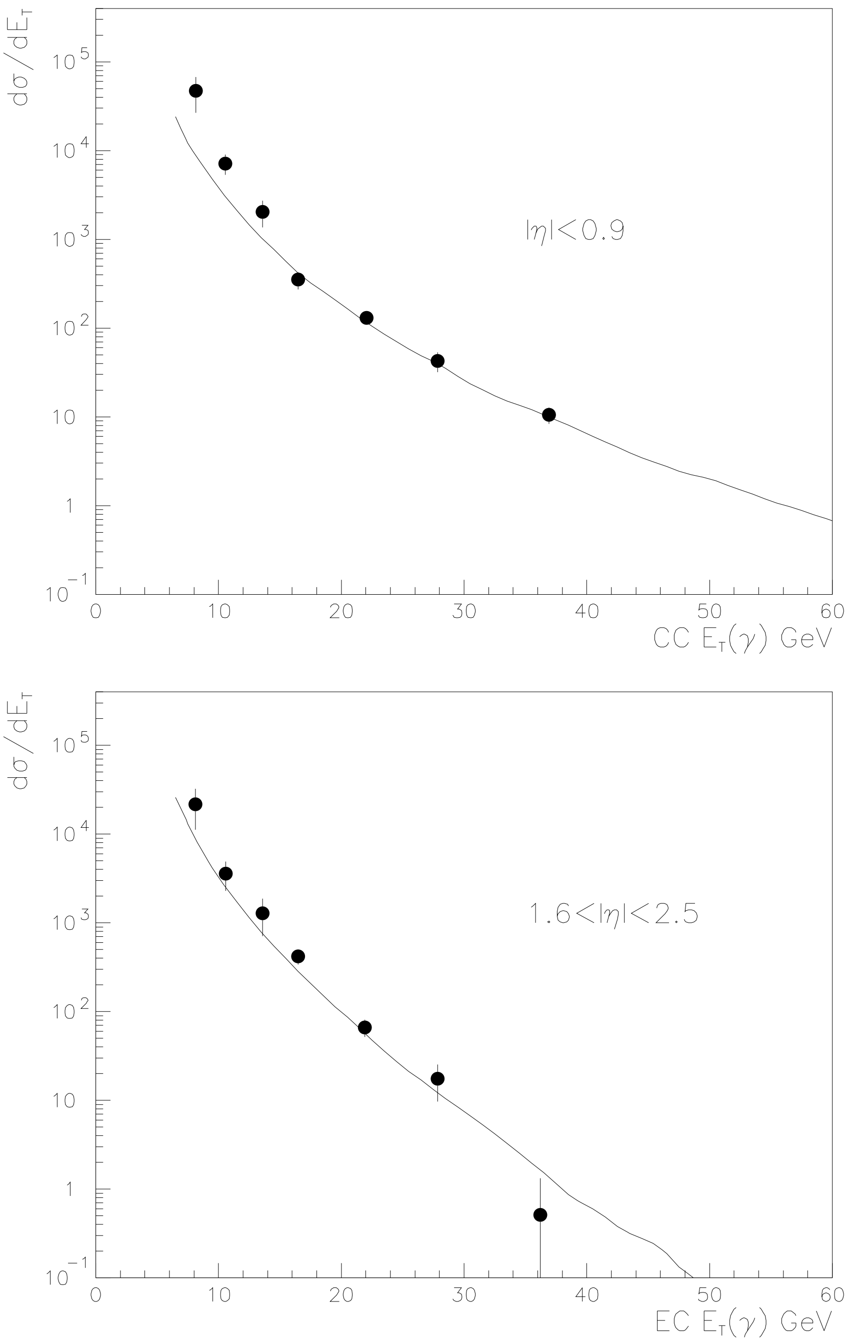

Figure 6: The isolated photon cross section, $d\sigma/dE_T\ d\eta$ vs. photon E_T for the central and forward rapidity regions. The errors are the total uncorrelated error and the curve is the theoretical prediction of CTEQ4M.

due to purity fitting (which includes statistical errors), the efficiency of the selection criteria, and the trigger efficiency. Contributions to the uncertainty from each of the sources is shown in Tables 3 and 5. The same data is plotted with the UA2 data and CTEQ5 as implemented by Vogelsang in Fig. 8 [5].

3 Significance

Both theoretical descriptions show relatively good agreement with the data. However, neither theory reproduces the data at lower E_T in the CC where the production cross section is higher than the theory.

A qualititive assessment of the agreement between data and theory is made by determining the χ^2 of the data with respect to the theory using the complete covariance matrix.

For each parameter in the cross section a fractional error matrix is determined taking all correlations into account. These error matrices are added together to produce a single fractional error matrix $\boldsymbol{A}$ which contains all correlated errors for each E_T bin. The total error matrix ($\boldsymbol{V}$) is given by

$$V_{ij} = A_{ij} T_i T_j + B_{ij} D_i D_j$$

where T_i and T_J are the theoretical cross sections in the ith and jth E_T bin, D_i and D_j are the measured cross section in the E_T bins, B_{ij} are the matrix elements of the fractional uncorrelated error matrix (which is diagonal). An overall χ^2 value is calculated using the equation

$$\boldsymbol{\chi^2 = (D - T)^{T}\, \overline{V}^{-1} (D - T).}$$

Using the data and theory in Fig. 7 we find a χ^2 value of 11.6 (7.72) for 7 degrees of freedom in the CC (EC). Therefore, the probability that the theory fits the data is 11.5% (35.8%) in the CC (EC).

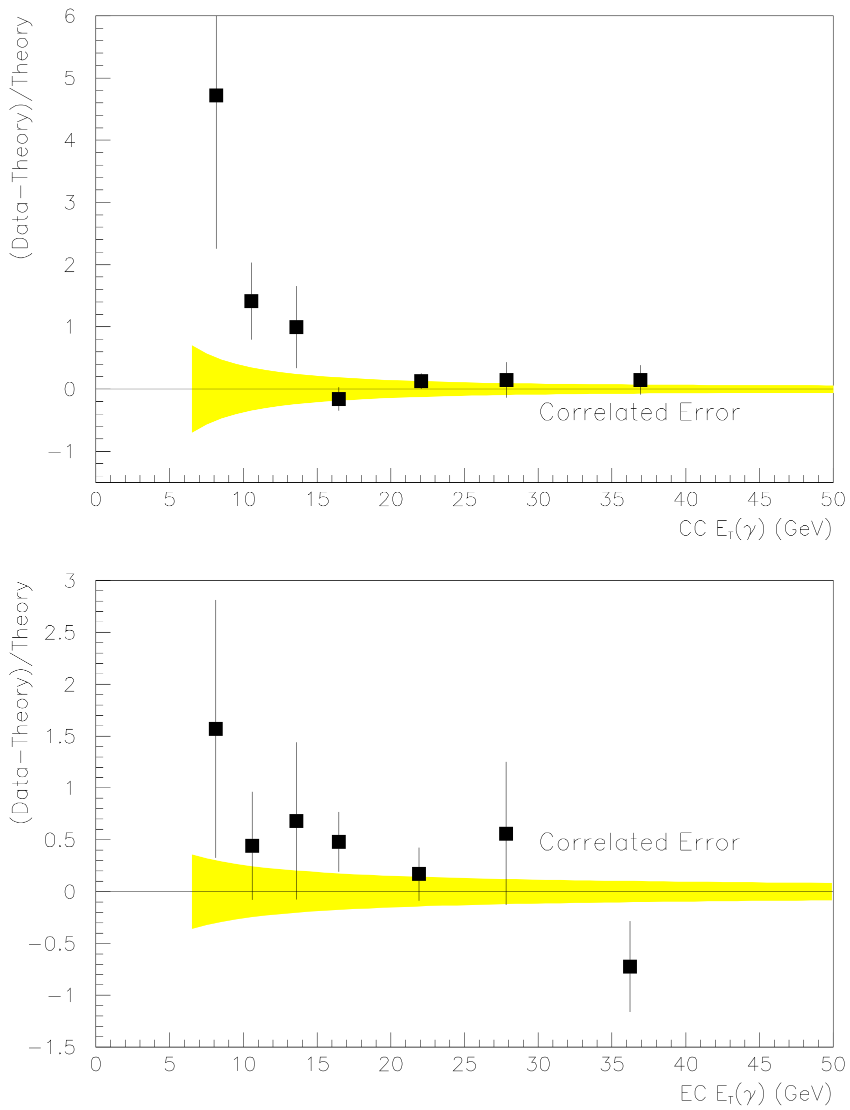

Figure 7: (Data-Theory)/Theory for the central (top) and forward (bottom) rapidity regions. The error bars indicate the uncorrelated uncertainty and the shaded region shows the correlated uncertainty.

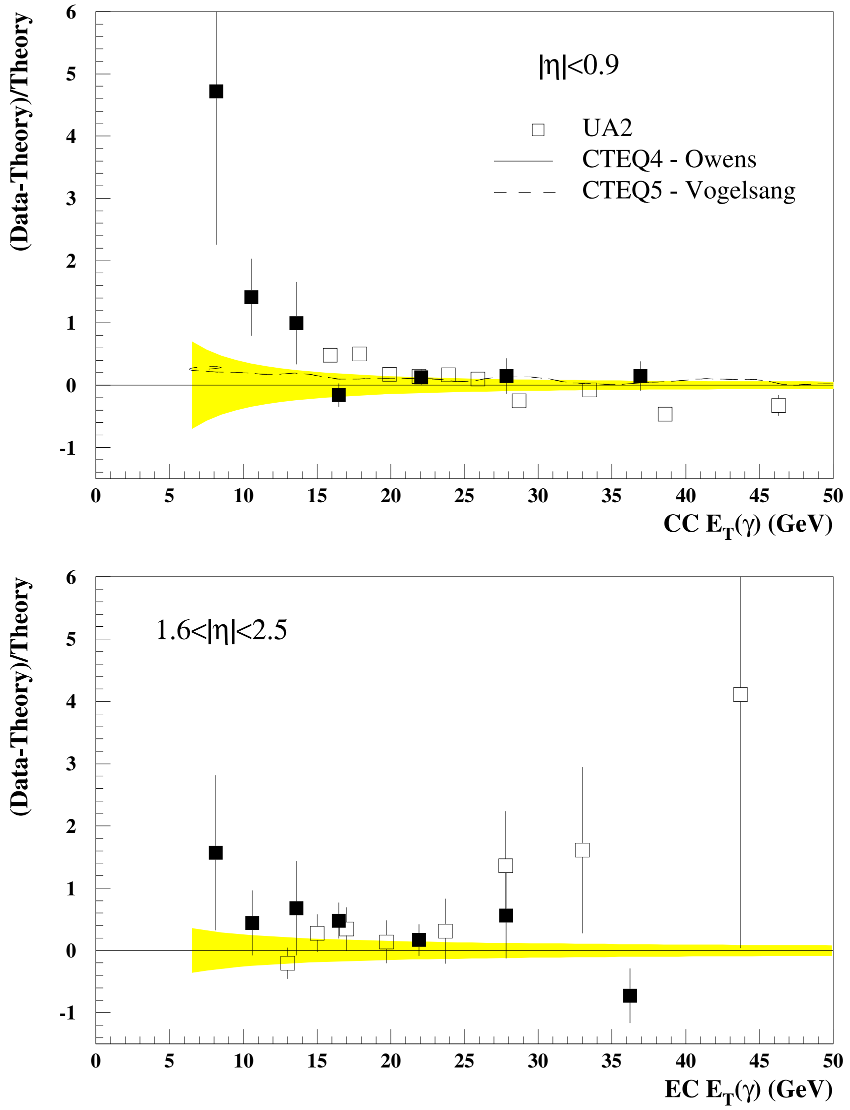

Figure 8: Same as Fig. 7 showing the UA2 data and CTEQ5 as implemented by Vogelsang. The errors for the UA2 data are statistical only, while the errors for the data in this analysis consist of all uncorrelated errors. The band shows the correlated uncertainty.

References

[1] "The Isolated Photon Cross Section at $\sqrt{s} = 1.8$," DØ Collaboration, *Phys. Rev. Lett.*, **84**, 2786, 2000.

[2] "The Isolated Photon Cross Section at $\sqrt{s} = 1.8$ TeV Using the Combined Run 1A/B Data Sample
S.L. Linn,DØ Note ♯ 3564, 1999.

[3] "A Measurement of the Isolated Direct Photon Cross Section at 630 GeV",
M. Strauss, M. Price, DØ Note ♯ 3699, 2000.

[4] J.F. Owens, Phys. Rev, **D42**, (1990) 61

[5] W. Vogelsang and A. Vogt, Nucl. Phys. **B453**, (1995) 334